Splitting methods for the solution of electron transport in semiconductors

Francesco Vecil

RICAM

Johannes Kepler Universität Linz, 07/10/08

Outline

Outline

Objects of the simulations

The goal of this work is a contribution to the numerical simulation of kinetic models for transistors.

Here we sketch the typical architecture of a **MOSFET**.
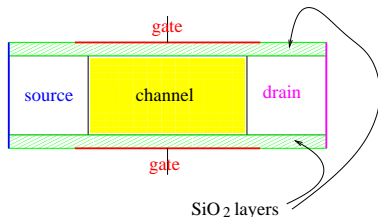
Figure: A **M**etal **O**xide **S**emiconductor **F**ield **E**ffect **T**ransistor.

Introduction | Numerical methods | Benchmark tests | Diode | nanoMOSFET
0000 | 000000000000 | 00000 | 000000000 | 0000000000

Introduction

Equations

Transport.

The Boltzmann Transport Equation (BTE) describes, at mesoscopic level, how the charge carriers move inside the object of study:

$$\frac{\partial f}{\partial t} + v \cdot \nabla_x f + \frac{F(t,x)}{m} \cdot \nabla_v f = \mathcal{Q}[f].$$

Force field.

Apart from the free motion, the charge carriers may be driven by the effect of a force field:

- self-consistent Poisson equation, in classical semiconductors;
- coupled Schrödinger-Poisson equation, in nanostructures.

Collisions.

The charge carriers may have collisions with other carriers, with the fixed lattice or with phonons (pseudo-particles describing the vibration of the lattice).

Equations

Transport.

The Boltzmann Transport Equation (BTE) describes, at mesoscopic level, how the charge carriers move inside the object of study:

$$\frac{\partial f}{\partial t} + v \cdot \nabla_x f + \frac{F(t,x)}{m} \cdot \nabla_v f = \mathcal{Q}[f].$$

Force field.

Apart from the free motion, the charge carriers may be driven by the effect of a force field:

- self-consistent Poisson equation, in classical semiconductors;
- coupled Schrödinger-Poisson equation, in nanostructures.

Collisions.

The charge carriers may have collisions with other carriers, with the fixed lattice or with phonons (pseudo-particles describing the vibration of the lattice).

Equations

Transport.

The Boltzmann Transport Equation (BTE) describes, at mesoscopic level, how the charge carriers move inside the object of study:

$$\frac{\partial f}{\partial t} + v \cdot \nabla_x f + \frac{F(t,x)}{m} \cdot \nabla_v f = \mathcal{Q}[f].$$

Force field.

Apart from the free motion, the charge carriers may be driven by the effect of a force field:

- self-consistent Poisson equation, in classical semiconductors;
- coupled Schrödinger-Poisson equation, in nanostructures.

Collisions.

The charge carriers may have collisions with other carriers, with the fixed lattice or with phonons (pseudo-particles describing the vibration of the lattice).

Transport

Two categories of transport equations are used.

Microscopic models.

At kinetic level the motion is described by a probabilistic magnitude f defined in the phase space (x, v), (x, p) or (x, k): the choice of the problem may make more suitable the use of the velocity v instead of the impulsion p or the wave vector k.

Macroscopic models.

The system does not depend on v or p or k; the magnitude describing the evolution just depends on time and position. Starting from the BTE, hydrodynamics or diffusion limits give Euler, Navier-Stokes, Spherical Harmonics Expansion, Energy-Transport or Drift-Diffusion systems.

Transport

Two categories of transport equations are used.

Microscopic models.

At kinetic level the motion is described by a probabilistic magnitude f defined in the phase space (x, v), (x, p) or (x, k): the choice of the problem may make more suitable the use of the velocity v instead of the impulsion p or the wave vector k.

Macroscopic models.

The system does not depend on v or p or k; the magnitude describing the evolution just depends on time and position. Starting from the BTE, hydrodynamics or diffusion limits give Euler, Navier-Stokes, Spherical Harmonics Expansion, Energy-Transport or Drift-Diffusion systems.

| Introduction | Numerical methods | Benchmark tests | Diode | nanoMOSFET |
| 000● | 000000000000 | 00000 | 000000000 | 0000000000 |

Introduction

Transport

Two categories of transport equations are used.

Microscopic models.

At kinetic level the motion is described by a probabilistic magnitude f defined in the phase space (x, v), (x, p) or (x, k): the choice of the problem may make more suitable the use of the velocity v instead of the impulsion p or the wave vector k.

Macroscopic models.

The system does not depend on v or p or k; the magnitude describing the evolution just depends on time and position. Starting from the BTE, hydrodynamics or diffusion limits give Euler, Navier-Stokes, Spherical Harmonics Expansion, Energy-Transport or Drift-Diffusion systems.

| Introduction | Numerical methods | Benchmark tests | Diode | nanoMOSFET |
| 0000 | ●○○○○○○○○○○○○ | ○○○○○ | ○○○○○○○○○ | ○○○○○○○○○○○ |

Splitting techniques

Outline

Introduction	Numerical methods	Benchmark tests	Diode	nanoMOSFET
0000	0●00000000000	00000	000000000	0000000000

Splitting techniques

Motivation

In this work, splitting techniques are used at different levels, namely:

- to split the Boltzmann Transport Equation into the solution of the transport part and the collisional part for separate, i.e. the **Time Splitting**:

$$\frac{\partial f}{\partial t} + v \cdot \nabla_x f + F \cdot \nabla_v f = \mathcal{Q}[f]$$

splits into

$$\frac{\partial f}{\partial t} + v \cdot \nabla_x f + F \cdot \nabla_v f = 0, \qquad \frac{\partial f}{\partial t} = \mathcal{Q}[f];$$

- to split the (x, v)-phase space in a collisionless context (**Dimensional Splitting**):

$$\frac{\partial f}{\partial t} + v \cdot \nabla_x f + F \cdot \nabla_v f = 0$$

splits into

$$\frac{\partial f}{\partial t} + v \cdot \nabla_x f = 0, \qquad \frac{\partial f}{\partial t} + F \cdot \nabla_v f = 0.$$

Motivation

In this work, splitting techniques are used at different levels, namely:

- to split the Boltzmann Transport Equation into the solution of the transport part and the collisional part for separate, i.e. the **Time Splitting**:

$$\frac{\partial f}{\partial t} + v \cdot \nabla_x f + F \cdot \nabla_v f = \mathcal{Q}[f]$$

splits into

$$\frac{\partial f}{\partial t} + v \cdot \nabla_x f + F \cdot \nabla_v f = 0, \qquad \frac{\partial f}{\partial t} = \mathcal{Q}[f];$$

- to split the (x, v)-phase space in a collisionless context (**Dimensional Splitting**):

$$\frac{\partial f}{\partial t} + v \cdot \nabla_x f + F \cdot \nabla_v f = 0$$

splits into

$$\frac{\partial f}{\partial t} + v \cdot \nabla_x f = 0, \qquad \frac{\partial f}{\partial t} + F \cdot \nabla_v f = 0.$$

Motivation

In this work, splitting techniques are used at different levels, namely:

- to split the Boltzmann Transport Equation into the solution of the transport part and the collisional part for separate, i.e. the **Time Splitting**:

$$\frac{\partial f}{\partial t} + v \cdot \nabla_x f + F \cdot \nabla_v f = \mathcal{Q}[f]$$

splits into

$$\frac{\partial f}{\partial t} + v \cdot \nabla_x f + F \cdot \nabla_v f = 0, \qquad \frac{\partial f}{\partial t} = \mathcal{Q}[f];$$

- to split the (x, v)-phase space in a collisionless context (**Dimensional Splitting**):

$$\frac{\partial f}{\partial t} + v \cdot \nabla_x f + F \cdot \nabla_v f = 0$$

splits into

$$\frac{\partial f}{\partial t} + v \cdot \nabla_x f = 0, \qquad \frac{\partial f}{\partial t} + F \cdot \nabla_v f = 0.$$

Introduction	Numerical methods	Benchmark tests	Diode	nanoMOSFET
0000	00●000000000	00000	000000000	0000000000

Splitting techniques

General framework

The (formal) exact solution of the linear PDE

$$\frac{\partial f}{\partial t} = Lf, \qquad f(t=0) = f^0$$

is

$$f(t) = e^{Lt} f^0.$$

If we can write the linear operator L as the sum of two linear operators,

$$L = L_1 + L_2,$$

then we may approximate the exact solution by solving for separate

$$\frac{\partial f}{\partial t} = L_1 f \qquad \text{and} \qquad \frac{\partial f}{\partial t} = L_2 f.$$

Several schemes are proposed for reconstructing the solution of the original PDE
from the solution of either blocks; a first order (in time) scheme is given by

$$\tilde{f}(t + \Delta t) = e^{L_2 \Delta t} e^{L_1 \Delta t} f(t),$$

while a second order (in time) scheme is given by

$$\tilde{f}(t + \Delta t) = e^{L_1 \frac{\Delta t}{2}} e^{L_2 \Delta t} e^{L_1 \frac{\Delta t}{2}} f(t).$$

General framework

The (formal) exact solution of the linear PDE

$$\frac{\partial f}{\partial t} = Lf, \qquad f(t = 0) = f^0$$

is

$$f(t) = e^{Lt}f^0.$$

If we can write the linear operator L as the sum of two linear operators,

$$L = L_1 + L_2,$$

then we may approximate the exact solution by solving for separate

$$\frac{\partial f}{\partial t} = L_1 f \qquad \text{and} \qquad \frac{\partial f}{\partial t} = L_2 f.$$

Several schemes are proposed for reconstructing the solution of the original PDE
from the solution of either blocks; a first order (in time) scheme is given by

$$\tilde{f}(t + \Delta t) = e^{L_2 \Delta t} e^{L_1 \Delta t} f(t),$$

while a second order (in time) scheme is given by

$$\tilde{f}(t + \Delta t) = e^{L_1 \frac{\Delta t}{2}} e^{L_2 \Delta t} e^{L_1 \frac{\Delta t}{2}} f(t).$$

General framework

The (formal) exact solution of the linear PDE

$$\frac{\partial f}{\partial t} = Lf, \qquad f(t=0) = f^0$$

is

$$f(t) = e^{Lt}f^0.$$

If we can write the linear operator L as the sum of two linear operators,

$$L = L_1 + L_2,$$

then we may approximate the exact solution by solving for separate

$$\frac{\partial f}{\partial t} = L_1 f \qquad \text{and} \qquad \frac{\partial f}{\partial t} = L_2 f.$$

Several schemes are proposed for reconstructing the solution of the original PDE from the solution of either blocks; a first order (in time) scheme is given by

$$\tilde{f}(t + \Delta t) = e^{L_2 \Delta t} e^{L_1 \Delta t} f(t),$$

while a second order (in time) scheme is given by

$$\tilde{f}(t + \Delta t) = e^{L_1 \frac{\Delta t}{2}} e^{L_2 \Delta t} e^{L_1 \frac{\Delta t}{2}} f(t).$$

Introduction
0000

Numerical methods
00●000000000

Benchmark tests
00000

Diode
000000000

nanoMOSFET
0000000000

Splitting techniques

General framework

The (formal) exact solution of the linear PDE

$$\frac{\partial f}{\partial t} = Lf, \qquad f(t=0) = f^0$$

is

$$f(t) = e^{Lt} f^0.$$

If we can write the linear operator L as the sum of two linear operators,

$$L = L_1 + L_2,$$

then we may approximate the exact solution by solving for separate

$$\frac{\partial f}{\partial t} = L_1 f \qquad \text{and} \qquad \frac{\partial f}{\partial t} = L_2 f.$$

Several schemes are proposed for reconstructing the solution of the original PDE from the solution of either blocks; a first order (in time) scheme is given by

$$\tilde{f}(t + \Delta t) = e^{L_2 \Delta t} e^{L_1 \Delta t} f(t),$$

while a second order (in time) scheme is given by

$$\tilde{f}(t + \Delta t) = e^{L_1 \frac{\Delta t}{2}} e^{L_2 \Delta t} e^{L_1 \frac{\Delta t}{2}} f(t).$$

Introduction	**Numerical methods**	Benchmark tests	Diode	nanoMOSFET
○○○○	○○○●○○○○○○○○	○○○○○	○○○○○○○○○	○○○○○○○○○○○○

Linear advection

Outline

Introduction	Numerical methods	Benchmark tests	Diode	nanoMOSFET
○○○○	○○○○○●○○○○○○○	○○○○○	○○○○○○○○○	○○○○○○○○○○○

Linear advection

Linear advection

We propose two schemes for solving the linear advection

$$\frac{\partial f}{\partial t} + v\frac{\partial f}{\partial x} = 0:$$

Semi-Lagrangian:

Directly integrate backward in the characteristic

Linear advection

We propose two schemes for solving the linear advection

$$\frac{\partial f}{\partial t} + v\frac{\partial f}{\partial x} = 0 :$$

Semi-Lagrangian:
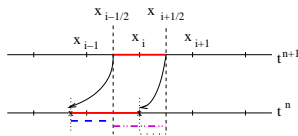
Directly integrate backward in the characteristic

Linear advection

Flux Balance Method:

Total mass conservation is forced. It is based on the idea of following backward the characteristics, but integral values are taken instead of point values:

The averages along the red segments are the same, because we have followed the characteristics backward.

FLUX BALANCE METHOD means evualuating the flux at time t^{n+1} from a balance of fluxes at previous time t^n :

–·–·–·–·– the average along the purple segment

– – – – – plus the average along the blue segment

········· minus the average along the green segment

Outline

Introduction	Numerical methods	Benchmark tests	Diode	nanoMOSFET
0000	000000000000	00000	000000000	0000000000

PWENO interpolations

Motivation

We need a **Pointwise** interpolation method which does not add spurious oscillations when high gradients appear, e.g. when a jump has to be transported.

Figure: Left: PWENO interpolation. Right: Lagrange interpolation.

Introduction	Numerical methods	Benchmark tests	Diode	nanoMOSFET
0000	000000000000	00000	000000000	000000000000

PWENO interpolations

Motivation

We need a **Pointwise** interpolation method which does not add spurious oscillations when high gradients appear, e.g. when a jump has to be transported.
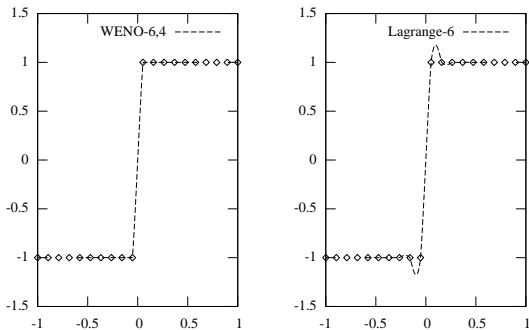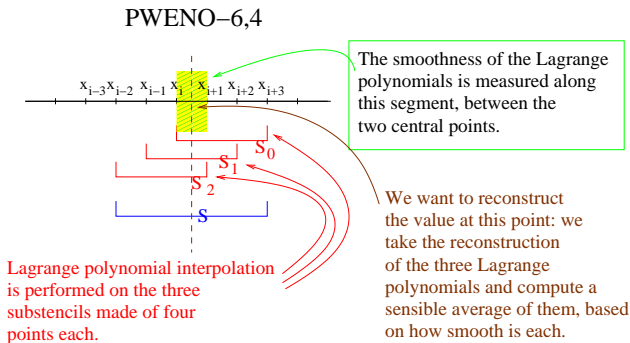

Figure: Left: PWENO interpolation. Right: Lagrange interpolation.

Introduction	Numerical methods	Benchmark tests	Diode	nanoMOSFET
○○○○	○○○○○○○○●○○○	○○○○○	○○○○○○○○○○	○○○○○○○○○○○○○

PWENO interpolations

Non-oscillatory properties

Essentially Non Oscillatory (ENO) methods are based on on a sensible average of Lagrange polynomial reconstructions.

We describe the case of PWENO-6,4: we take a stencil of six points and divide it into three substencils of four points:

PWENO−6,4

The smoothness of the Lagrange polynomials is measured along this segment, between the two central points.

We want to reconstruct the value at this point: we take the reconstruction of the three Lagrange polynomials and compute a sensible average of them, based on how smooth is each.

Lagrange polynomial interpolation is performed on the three substencils made of four points each.

Non-oscillatory properties

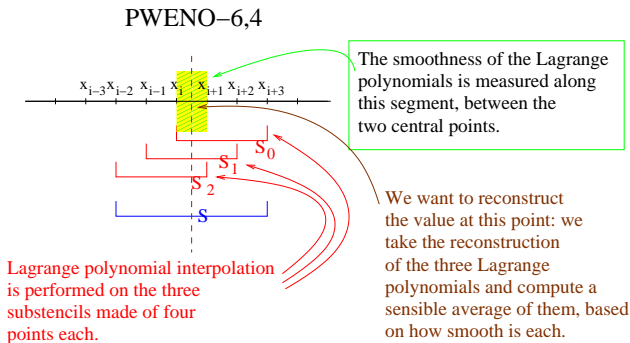Essentially Non Oscillatory (ENO) methods are based on on a sensible average of Lagrange polynomial reconstructions.

We describe the case of PWENO-6,4: we take a stencil of six points and divide it into three substencils of four points:

PWENO−6,4

The smoothness of the Lagrange polynomials is measured along this segment, between the two central points.

We want to reconstruct the value at this point: we take the reconstruction of the three Lagrange polynomials and compute a sensible average of them, based on how smooth is each.

Lagrange polynomial interpolation is performed on the three substencils made of four points each.

Introduction	Numerical methods	Benchmark tests	Diode	nanoMOSFET
○○○○	○○○○○○○○○●○○	○○○○○	○○○○○○○○○	○○○○○○○○○○○

PWENO interpolations

The average

If we note $p_r(x)$ the Lagrange polynomials, PWENO reconstruction reads

$$p_{PWENO}(x) = \omega_0(x)p_0(x) + \omega_1(x)p_1(x) + \omega_2(x)p_2(x).$$

Convex combination.

The convex combination $\{\omega_r(x)\}_r$ must penalize the substencils $\mathcal{S}_r$ in which the $p_r(x)$ have high derivatives.

Smoothness indicators

In order to decide which substencils $\mathcal{S}_r$ are "regular" and which ones are not, we have to introduce the smoothness indicators: we use a weighted sum of the L^2-norms of the Lagrange polynomials $p_r(x)$ to measure their regularity close to the reconstruction point x. The following smoothness indicators have been proposed by Jiang and Shu:

$$\beta_r = \Delta x \left\| \frac{dp_r}{dx} \right\|_{L^2_{(x_i,x_{i+1})}} + \Delta x^3 \left\| \frac{d^2 p_r}{dx^2} \right\|_{L^2_{(x_i,x_{i+1})}} + \Delta x^5 \left\| \frac{d^3 p_r}{dx^3} \right\|_{L^2_{(x_i,x_{i+1})}}.$$

Introduction	Numerical methods	Benchmark tests	Diode	nanoMOSFET
0000	000000000●00	00000	000000000	0000000000

PWENO interpolations

The average

If we note $p_r(x)$ the Lagrange polynomials, PWENO reconstruction reads

$$p_{PWENO}(x) = \omega_0(x)p_0(x) + \omega_1(x)p_1(x) + \omega_2(x)p_2(x).$$

Convex combination.

The convex combination $\{\omega_r(x)\}_r$ must penalize the substencils $\mathcal{S}_r$ in which the $p_r(x)$ have high derivatives.

Smoothness indicators

In order to decide which substencils $\mathcal{S}_r$ are "regular" and which ones are not, we have to introduce the smoothness indicators: we use a weighted sum of the L^2-norms of the Lagrange polynomials $p_r(x)$ to measure their regularity close to the reconstruction point x. The following smoothness indicators have been proposed by Jiang and Shu:

$$\beta_r = \Delta x \left\| \frac{dp_r}{dx} \right\|_{L^2_{(x_i, x_{i+1})}} + \Delta x^3 \left\| \frac{d^2 p_r}{dx^2} \right\|_{L^2_{(x_i, x_{i+1})}} + \Delta x^5 \left\| \frac{d^3 p_r}{dx^3} \right\|_{L^2_{(x_i, x_{i+1})}}.$$

Introduction	Numerical methods	Benchmark tests	Diode	nanoMOSFET
0000	000000000●00	00000	000000000	0000000000

PWENO interpolations

The average

If we note $p_r(x)$ the Lagrange polynomials, PWENO reconstruction reads

$$p_{PWENO}(x) = \omega_0(x)p_0(x) + \omega_1(x)p_1(x) + \omega_2(x)p_2(x).$$

Convex combination.

The convex combination $\{\omega_r(x)\}_r$ must penalize the substencils $\mathcal{S}_r$ in which the $p_r(x)$ have high derivatives.

Smoothness indicators

In order to decide which substencils $\mathcal{S}_r$ are "regular" and which ones are not, we have to introduce the smoothness indicators: we use a weighted sum of the L^2-norms of the Lagrange polynomials $p_r(x)$ to measure their regularity close to the reconstruction point x. The following smoothness indicators have been proposed by Jiang and Shu:

$$\beta_r = \Delta x \left\| \frac{dp_r}{dx} \right\|_{L^2_{(x_i,x_{i+1})}} + \Delta x^3 \left\| \frac{d^2 p_r}{dx^2} \right\|_{L^2_{(x_i,x_{i+1})}} + \Delta x^5 \left\| \frac{d^3 p_r}{dx^3} \right\|_{L^2_{(x_i,x_{i+1})}}.$$

High order reconstruction

Admit for now that the convex combination is given by the normalization
$\omega_r(x) = \frac{\tilde{\omega}_r(x)}{\sum_{s=0}^{2} \tilde{\omega}_s(x)}$ of the protoweights $\tilde{\omega}_r(x)$ defined this way:

$$\tilde{\omega}_r(x) = \frac{d_r(x)}{(\epsilon + \beta_r)^2}.$$

Regular reconstruction

Suppose that all the β_r are equal; then we have

$$\omega_r(x) = d_r(x).$$

The optimal order is achieved by Lagrange reconstruction $p_{Lagrange}(x)$ in the whole
stencil $\mathcal{S}$, so if we define $d_r(x)$ to be the polynomials such that

$$p_{Lagrange}(x) = d_0(x)p_0(x) + d_1(x)p_1(x) + d_2(x)p_2(x),$$

then we have achieved the optimal order because $p_{PWENO}(x) = p_{Lagrange}(x)$.

High order reconstruction

Admit for now that the convex combination is given by the normalization
$\omega_r(x) = \frac{\tilde{\omega}_r(x)}{\sum_{s=0}^2 \tilde{\omega}_s(x)}$ of the protoweights $\tilde{\omega}_r(x)$ defined this way:

$$\tilde{\omega}_r(x) = \frac{d_r(x)}{(\epsilon + \beta_r)^2}.$$

Regular reconstruction

Suppose that all the β_r are equal; then we have

$$\omega_r(x) = d_r(x).$$

The optimal order is achieved by Lagrange reconstruction $p_{Lagrange}(x)$ in the whole
stencil $\mathcal{S}$, so if we define $d_r(x)$ to be the polynomials such that

$$p_{Lagrange}(x) = d_0(x)p_0(x) + d_1(x)p_1(x) + d_2(x)p_2(x),$$

then we have achieved the optimal order because $p_{PWENO}(x) = p_{Lagrange}(x)$.

High order reconstruction

Admit for now that the convex combination is given by the normalization
$\omega_r(x) = \frac{\tilde{\omega}_r(x)}{\sum_{s=0}^{2} \tilde{\omega}_s(x)}$ of the protoweights $\tilde{\omega}_r(x)$ defined this way:

$$\tilde{\omega}_r(x) = \frac{d_r(x)}{(\epsilon + \beta_r)^2}.$$

High gradients

Otherwise, suppose for instance that β_0 is high order than the other ones: in this case $\mathcal{S}_0$ is penalized and most of the reconstruction is carried by the other more "regular" substencils.

Outline

The system

We solve a Vlasov equation with given potential and a linear relaxation-time operator as collision operator by time (linear) splitting to decouple the Vlasov part and the Boltzmann part, and recursively dimensional splitting to divide the x-advection from the v-advection:

$$\frac{\partial f}{\partial t} + v \frac{\partial f}{\partial x} - \frac{d\left(\frac{x^2}{2}\right)}{dx} \frac{\partial f}{\partial v} = \frac{1}{\tau}\left[\frac{1}{\pi} e^{-\frac{v^2}{2}} \rho - f\right], \qquad f(0, x) = f_0(x).$$

We expect the solution to rotate (due to the Vlasov part and the potential) and to converge to an equilibrium (due to collisions) given by

$$f_s = \frac{\text{mass}(f)}{\pi^2} \exp\left(-\frac{x^2 + v^2}{2}\right).$$

Introduction	Numerical methods	**Benchmark tests**	Diode	nanoMOSFET
○○○○	○○○○○○○○○○○○	○○●○○	○○○○○○○○○	○○○○○○○○○○

Vlasov with confining potential

Setting up initial conditions

We perform tests with three initial conditions, more or less close to the equilibrium; the relaxation time is set $\tau = 3.5$:

$$
\begin{aligned}
f_0^{(1)} &= Z_1 \sin^2\left(\frac{x}{2}\right) e^{-\frac{x^2+v^2}{2}} \\
f_0^{(2)} &= Z_2 \sin^2\left(\frac{x}{2}\right) \sin^2\left(\frac{v}{2}\right) e^{-\frac{x^2+v^2}{2}} \\
f_0^{(3)} &= Z_3 \left[1 + 0.05 \sin^2\left(\frac{x}{2}\right)\right] e^{-\frac{x^2+v^2}{2}}.
\end{aligned}
$$

Entropies

The global and local relative entropies are defined this way:

$$
\begin{aligned}
H[f;f_s] &= \int_{\mathbb{R}} \int_{\mathbb{R}} \frac{|f - f_s|^2}{f_s} \, dv dx \\
\tilde{H}[f;\rho M_1] &= \int_{\mathbb{R}} \int_{\mathbb{R}} \frac{|f - \rho M_1|^2}{f_s} \, dv dx.
\end{aligned}
$$

Introduction	Numerical methods	**Benchmark tests**	Diode	nanoMOSFET
0000	000000000000	0000●0	000000000	0000000000

Vlasov-Poisson

Outline

Two-stream instability

The problem

We set the problem in a collisionless context. The force field is self-consistently computed through a Poisson equation. Equations are normalized, periodic boundary conditions are taken for both the transport and the potential.

$$\frac{\partial f}{\partial t} + v\frac{\partial f}{\partial x} - \frac{\partial \Phi}{\partial x}\frac{\partial f}{\partial v} = 0$$

$$\frac{\partial^2 \Phi}{\partial x^2} = 1 - \int_{\mathbb{R}} f dv$$

$$f(t=0, x, v) = f_{eq}(v)\left[1 + 0.01\left(\frac{\cos(2kx) + \cos(3kx)}{1.2} + \cos(kx)\right)\right].$$

As initial condition, we perturb the equilibrium-state given by

$$f_{eq}(v) = K(1 + v^2)e^{-\frac{v^2}{2}},$$

K being a normalization factor.

Outline

| Introduction | Numerical methods | Benchmark tests | **Diode** | nanoMOSFET |
| 0000 | 000000000000 | 00000 | 0●00000000 | 0000000000 |

Overview

The model

We describe via the Boltzmann Transport Equation the transport/collision in an electronic device

$$\frac{\partial f}{\partial t} + \frac{1}{\hbar}\nabla_k \varepsilon \cdot \nabla_x f - \frac{q}{\hbar}E \cdot \nabla_k f = \mathcal{Q}[f]$$

$$\Delta \Phi = \frac{q}{\epsilon_0}\left[\rho[f] - N_D\right], \qquad E = -\nabla_x \Phi$$

$$f_0(x,k) = N_D(x)M(k),$$

where the band structure is given in the parabolic approximation

$$\varepsilon(k) = \frac{\hbar^2 |k|^2}{2m_*},$$

m_* being the Silicon effective mass.

The collision operator

The collision operator takes into account the scattering of the carriers with acoustic phonons, in the elastic approximation, and with optical phonons, with a single frequency ω. Therefore the operator reads, in the low-density approximation:

$$\mathcal{Q}[f] = \int_{\mathbb{R}^3} \left[S(k', k) f(t, x, k') - S(k, k') f(t, x, k) \right] dk',$$

where the scattering rate is given by

$$
\begin{aligned}
S(k, k') &= K \left[(n_q + 1)\delta(\epsilon(k') - \epsilon(k) + \hbar\omega) + n_q \delta(\epsilon(k') - \epsilon(k) - \hbar\omega) \right] \\
&+ K_0 \delta(\epsilon(k') - \epsilon(k)).
\end{aligned}
$$

| Introduction | Numerical methods | Benchmark tests | **Diode** | nanoMOSFET |
| 0000 | 000000000000 | 00000 | 000●00000 | 0000000000 |

Numerics

Outline

Introduction	Numerical methods	Benchmark tests	**Diode**	nanoMOSFET
0000	000000000000	00000	0000●0000	0000000000

Numerics

Adimensionalization

The system is reduced to dimensionless magnitudes in order to improve numerical results by making the computer perform calculations on numbers of order 1. Then splitting schemes are applied to solve for separate transport and collision, and dimensional splitting is applied to separate x-dimension from k_1-dimension.

adim.	parameter	400 nm device	50 nm device
$\tilde{k} = k^* k$	$k^* = \frac{\sqrt{2m^* k_B T_L}}{\hbar}$	$4.65974 \times 10^8 m^{-1}$	$4.65974 \times 10^8 m^{-1}$
$\tilde{x} = l^* x$	$l^* =$ device length	$1\ \mu m$	$250\ nm$
$\tilde{t} = t^* t$	$t^* =$ typical time	$1\ ps = 10^{-12}s$	$1\ ps = 10^{-12}s$
$\tilde{V}(\tilde{x}) = V^* V(x)$	$V^* =$ typical Vbias	$1V$	$1V$
$\tilde{E}(\tilde{x}) = E^* E(x)$	$E^* = \frac{1}{10} \frac{V^*}{l^*}$	$100000 V m^{-1}$	$400000 V m^{-1}$
$\tilde{\varepsilon}(\tilde{k}) = \varepsilon^* \varepsilon(k)$	$\epsilon^* = \frac{\hbar^2 k^{*2}}{2m^*}$	$4.14195e - 21$	$4.14195e - 21$
$\tilde{\rho}(\tilde{x}) = \rho^* \rho(x)$	$\rho^* = \left(\frac{2m^* k_B T_L}{\hbar}\right)^{3/2}$	1.01178×10^{26}	1.01178×10^{26}
$\tilde{j}(\tilde{x}) = j^* j(x)$	$j^* = \frac{1}{l^{*2} t^*}$	10^{24}	1.6×10^{25}
$\tilde{u}(\tilde{x}) = u^* u(x)$	$u^* = \frac{l^*}{t^*}$	10^6	250000
$\tilde{W}(\tilde{x}) = W^* W(x)$	$W^* = (l^*/t^*)^2$	10^{12}	6.25×10^{10}

.

| Introduction | Numerical methods | Benchmark tests | **Diode** | nanoMOSFET |
| 0000 | 000000000000 | 00000 | 000000000000 | 0000000000 |

Numerics

Collision integraion

The solution of the collisions is achieved when we are able to solve the following integrals (in dimensionless units):

$$
\begin{aligned}
\mathcal{Q}^+[f] &= c_0\pi \int_{-\sqrt{\gamma_0(k)}}^{\sqrt{\gamma_0(k)}} f\left(k'_1, \sqrt{\gamma_0(k) - k'^2_1}\right) dk'_1 \\
&+ c_+\pi \int_{-\sqrt{\gamma_+(k)}}^{\sqrt{\gamma_+(k)}} f\left(k'_1, \sqrt{\gamma_+(k) - k'^2_1}\right) dk'_1 \\
&+ \chi_{\left\{\gamma_-(k)>0\right\}} c_-\pi \int_{-\sqrt{\gamma_-(k)}}^{\sqrt{\gamma_-(k)}} f\left(k'_1, \sqrt{\gamma_-(k) - k'^2_1}\right) dk'_1
\end{aligned}
$$

with $\gamma_0(k) = \varepsilon(k)$, $\gamma_+(k) = \varepsilon(k) + \dfrac{\hbar\omega}{\varepsilon^*}$, $\gamma_-(k) = \varepsilon(k) - \dfrac{\hbar\omega}{\varepsilon^*}$, and

$$
\mathcal{Q}^-[f] = c_0 2\pi\sqrt{\gamma_0(k)}f(k) + \chi_{\left\{\gamma_-(k)>0\right\}} c_+ 2\pi\sqrt{\gamma_-(k)}f(k) + c_- 2\pi\sqrt{\gamma_+(k)}f(k).
$$

Introduction	Numerical methods	Benchmark tests	Diode	nanoMOSFET
○○○○	○○○○○○○○○○○○	○○○○○	○○○○○○○●○○	○○○○○○○○○○○○

Numerics

Collision integraion

For integrating along the $[-\sqrt{\gamma}, \sqrt{\gamma}]$-segment following a semicircle in the $\left(k_1, \sqrt{k_2^2 + k_3^2}\right)$-plane, we have adopted as strategy a plain linear interpolation using the values of the two nearest points along the vertical lines. Other more sofisticated strategies have not significantly improved the results.

Introduction	Numerical methods	Benchmark tests	**Diode**	nanoMOSFET
0000	000000000000	00000	0000000●0	0000000000

Experiments

Outline

Multifrequency phonons

We present the results relative to a device where phonons are not single-frequency:
the structure of the solver allows an easy implementation of such model.

Outline

The model

We afford the simulation of a nanoscaled MOSFET.
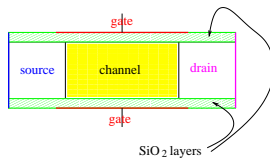
Dimensional coupling

x-dimension is longer than z-dimension, therefore we adopt a different description:

- along x-dimension electrons behave like particles, their movement being described by the Boltzmann Transport Equation;

- along z-dimension electrons confined in a potential well behave like waves, moreover they are supposed to be at equilibrium, therefore their state is given by the stationary-state Schrödinger equation.

The model

Subband decomposition

Electrons in different energy levels, also called *sub-bands*, another name for the eigenvalues of the Schrödinger equation, have to be considered independent populations, so that we have to transport them for separate.

Coupling between dimensions

Dimensions and subbands are coupled in the Poisson equation for the computation of the electrostatic field in the expression of the total density.

Coupling between subbands

Subbands are also coupled in the scattering operator, where the carriers are allowed to jump from an energy level to another one.

The model

Subband decomposition

Electrons in different energy levels, also called *sub-bands*, another name for the eigenvalues of the Schrödinger equation, have to be considered independent populations, so that we have to transport them for separate.

Coupling between dimensions

Dimensions and subbands are coupled in the Poisson equation for the computation of the electrostatic field in the expression of the total density.
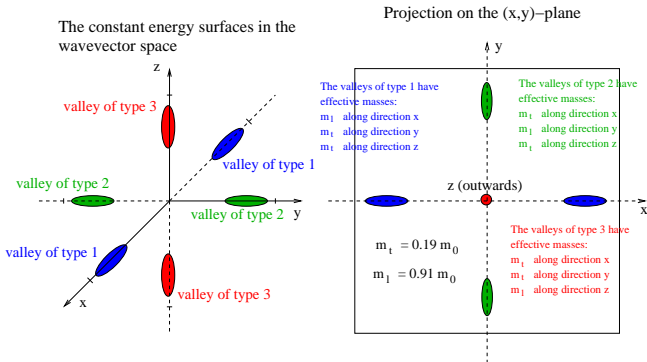
Coupling between subbands

Subbands are also coupled in the scattering operator, where the carriers are allowed to jump from an energy level to another one.

The model

Subband decomposition

Electrons in different energy levels, also called *sub-bands*, another name for the eigenvalues of the Schrödinger equation, have to be considered independent populations, so that we have to transport them for separate.

Coupling between dimensions

Dimensions and subbands are coupled in the Poisson equation for the computation of the electrostatic field in the expression of the total density.

Coupling between subbands

Subbands are also coupled in the scattering operator, where the carriers are allowed to jump from an energy level to another one.

Introduction
○○○○

Numerical methods
○○○○○○○○○○○○○

Benchmark tests
○○○○○

Diode
○○○○○○○○○○○

nanoMOSFET
○○○○●○○○○○○

Geometry

Bandstructure

The three valleys

The Si bandstructure presents six minima in the first Brillouin zone:

The constant energy surfaces in the wavevector space

Projection on the (x,y)–plane

valley of type 3

valley of type 1

valley of type 2

valley of type 2   y

valley of type 1

valley of type 3

z (outwards)

The valleys of type 1 have effective masses:
m_l along direction x
m_t along direction y
m_t along direction z

The valleys of type 2 have effective masses:
m_t along direction x
m_l along direction y
m_t along direction z

The valleys of type 3 have effective masses:
m_t along direction x
m_t along direction y
m_l along direction z

$m_t = 0.19\, m_0$

$m_l = 0.91\, m_0$

The axes of the ellipsoids are disposed along the *x*, *y* and *z* axes of the reciprocal lattice. The three minima have the same value, therefore there is no gap.

Introduction	Numerical methods	Benchmark tests	Diode	nanoMOSFET
○○○○	○○○○○○○○○○○○	○○○○○	○○○○○○○○○	○○○○●○○○○○

Geometry

Bandstructure

Non-parabolicity

The bandstructure around the three minima can be expanded following the Kane non-parabolic approximation:

$$
\epsilon_\nu^{kin} \;=\; \frac{\hbar^2}{1 + \sqrt{1 + 2\tilde{\alpha}_\nu \hbar^2 \left(\frac{k_x^2}{m_\nu^x} + \frac{k_y^2}{m_\nu^y} \right)}} \left(\frac{k_x^2}{m_\nu^x} + \frac{k_y^2}{m_\nu^y} \right),
$$

where $m_\nu^{\{x,y\}}$ are the axes of the ellipsoids (called *effective masses*) of the νth valley along x and y directions, and the $\tilde{\alpha}_\nu$ are known as Kane dispersion factors.

The simplest case: one-valley, parabolic

$$
\epsilon^{kin} \;=\; \frac{\hbar^2 |k|^2}{2m_*},
$$

with m_* an average value between the effective masses.

Introduction	Numerical methods	Benchmark tests	Diode	nanoMOSFET
0000	000000000000	00000	000000000	0000●00000

Geometry

Bandstructure

Non-parabolicity

The bandstructure around the three minima can be expanded following the Kane non-parabolic approximation:

$$\epsilon_{\nu}^{kin} = \frac{\hbar^2}{1 + \sqrt{1 + 2\tilde{\alpha}_{\nu}\hbar^2 \left(\frac{k_x^2}{m_{\nu}^x} + \frac{k_y^2}{m_{\nu}^y} \right)}} \left(\frac{k_x^2}{m_{\nu}^x} + \frac{k_y^2}{m_{\nu}^y} \right),$$

where $m_{\nu}^{\{x,y\}}$ are the axes of the ellipsoids (called *effective masses*) of the νth valley along x and y directions, and the $\tilde{\alpha}_{\nu}$ are known as Kane dispersion factors.

The simplest case: one-valley, parabolic

$$\epsilon^{kin} = \frac{\hbar^2 |k|^2}{2m_*},$$

with m_* an average value between the effective masses.

Introduction | Numerical methods | Benchmark tests | Diode | nanoMOSFET
0000 | 000000000000 | 00000 | 000000000 | 000000●0000

Mathematical model

Outline

The model

BTE

The Boltzmann Transport Equation (one for each band and for each valley) reads

$$\frac{\partial f_{\nu,p}}{\partial t} + \frac{1}{\hbar}\nabla_k \epsilon_\nu^{kin} \cdot \nabla_x f_{\nu,p} - \frac{1}{\hbar}\nabla_x \epsilon_{\nu,p}^{pot} \cdot \nabla_k f_{\nu,p} = \mathcal{Q}_{\nu,p}[f], \qquad f_{\nu,p}(t=0) = \rho_{\nu,p}^{eq}M.$$

Schrödinger-Poisson block

$$-\frac{\hbar^2}{2}\frac{d}{dz}\left[\frac{1}{m_\nu}\frac{d\chi_{\nu,p}[V]}{dz}\right] - q\left(V + V_c\right)\chi_{\nu,p}[V] = \epsilon_{\nu,p}^{pot}[V]\chi_{\nu,p}[V]$$

$\{\chi_{\nu,p}\}_p \subseteq H_o^1(0,l_z)$ orthonormal basis

$$-\mathrm{div}\left[\varepsilon_R\nabla V\right] = -\frac{q}{\varepsilon_0}\left(\sum_{\nu,p}\rho_{\nu,p}|\chi_{\nu,p}[V]|^2 - N_D\right)$$

plus boundary conditions.

These equations cannot be decoupled because we need the eigenfunctions to compute the potential (in the expression of the total density), and we need the potential to compute the eigenfunctions.

The model

BTE

The Boltzmann Transport Equation (one for each band and for each valley) reads

$$\frac{\partial f_{\nu,p}}{\partial t} + \frac{1}{\hbar} \nabla_k \epsilon_\nu^{kin} \cdot \nabla_x f_{\nu,p} - \frac{1}{\hbar} \nabla_x \epsilon_{\nu,p}^{pot} \cdot \nabla_k f_{\nu,p} = \mathcal{Q}_{\nu,p}[f], \qquad f_{\nu,p}(t=0) = \rho_{\nu,p}^{eq} M.$$

Schrödinger-Poisson block

$$-\frac{\hbar^2}{2} \frac{d}{dz} \left[\frac{1}{m_\nu} \frac{d\chi_{\nu,p}[V]}{dz} \right] - q\left(V + V_c\right) \chi_{\nu,p}[V] = \epsilon_{\nu,p}^{pot}[V] \chi_{\nu,p}[V]$$

$$\left\{ \chi_{\nu,p} \right\}_p \subseteq H_o^1(0, l_z) \text{ orthonormal basis}$$

$$-\text{div}\left[\varepsilon_R \nabla V\right] = -\frac{q}{\varepsilon_0} \left(\sum_{\nu,p} \rho_{\nu,p} |\chi_{\nu,p}[V]|^2 - N_D \right)$$

plus boundary conditions.

These equations cannot be decoupled because we need the eigenfunctions to compute the potential (in the expression of the total density), and we need the potential to compute the eigenfunctions.

The model

The collision operator

The collision operator takes into account the electron-optical phonon scattering mechanism. It reads

$$\mathcal{Q}_{\nu,p}[f] = \sum_{s} \sum_{\nu',p'} \int_{\mathbb{R}^2} \left[S^s_{(\nu',p',k')\to(\nu,p,k)} f_{\nu',p'}(k') - S^s_{(\nu,p,k)\to(\nu',p',k')} f_{\nu,p}(k) \right] dk' :$$

every S^s represents a different interaction, which may be elastic or inelastic, intra-valley or inter-valley. Each of them is inter-band.

Structure of the S^s

Each of the S^s consists of a constant, an overlap integral and a delta for the exchange of energy:

$$S^s_{(\nu,p,k)\to(\nu',p',k')} = C_{\nu,\nu'} \int_0^{l_z} |\chi_{\nu,p}|^2 |\chi_{\nu',p'}|^2 dz \, \delta \left(\epsilon^{tot}_{\nu',p'}(k') - \epsilon^{tot}_{\nu,p}(k) \pm \text{some energy} \right).$$

The model

The collision operator

The collision operator takes into account the electron-optical phonon scattering mechanism. It reads

$$\mathcal{Q}_{\nu,p}[f] = \sum_{s} \sum_{\nu',p'} \int_{\mathbb{R}^2} \left[S^s_{(\nu',p',k') \to (\nu,p,k)} f_{\nu',p'}(k') - S^s_{(\nu,p,k) \to (\nu',p',k')} f_{\nu,p}(k) \right] dk' :$$

every S^s represents a different interaction, which may be elastic or inelastic, intra-valley or inter-valley. Each of them is inter-band.

Structure of the S^s

Each of the S^s consists of a constant, an overlap integral and a delta for the exchange of energy:

$$S^s_{(\nu,p,k) \to (\nu',p',k')} = C_{\nu,\nu'} \int_0^{l_z} |\chi_{\nu,p}|^2 |\chi_{\nu',p'}|^2 dz \, \delta \left(\epsilon^{tot}_{\nu',p'}(k') - \epsilon^{tot}_{\nu,p}(k) \pm \text{some energy} \right).$$

Introduction   Numerical methods   Benchmark tests   Diode   nanoMOSFET
0000   000000000000   00000   000000000   00000000000
Newton schemes for the Schrödinger-Poisson block

Outline

Introduction   Numerical methods   Benchmark tests   Diode   nanoMOSFET
○○○○   ○○○○○○○○○○○○   ○○○○○   ○○○○○○○○○   ○○○○○○○○○○●
Newton schemes for the Schrödinger-Poisson block

The Newton scheme

The functional

Solving the Schrödinger-Poisson block

$$-\frac{\hbar^2}{2}\frac{d}{dz}\left[\frac{1}{m_\nu}\frac{d\chi_{\nu,p}[V]}{dz}\right] - q\left(V + V_c\right)\chi_{\nu,p}[V] = \epsilon_{\nu,p}^{pot}[V]\chi_{\nu,p}[V]$$

$$-\text{div}\left[\varepsilon_R\nabla V\right] = -\frac{q}{\varepsilon_0}\left(\sum_{\nu,p}\rho_{\nu,p}|\chi_{\nu,p}[V]|^2 - N_D\right)$$

is equivalt to minimizing, under the constraints of the Schrödinger equation, the functional $P[V]$

$$P[V] = -\text{div}\left(\varepsilon_R\nabla V\right) + \frac{q}{\varepsilon_0}\left(\sum_{\nu,p}\rho_{\nu,p}|\chi_{\nu,p}[V]|^2 - N_D\right),$$

The scheme

which is achieved by means of a Newton scheme

$$dP(V^{old}, V^{new} - V^{old}) = -P[V^{old}].$$

The Newton scheme

The functional

Solving the Schrödinger-Poisson block

$$-\frac{\hbar^2}{2}\frac{d}{dz}\left[\frac{1}{m_\nu}\frac{d\chi_{\nu,p}[V]}{dz}\right] - q\left(V + V_c\right)\chi_{\nu,p}[V] = \epsilon_{\nu,p}^{pot}[V]\chi_{\nu,p}[V]$$

$$-\text{div}\left[\varepsilon_R \nabla V\right] = -\frac{q}{\varepsilon_0}\left(\sum_{\nu,p}\rho_{\nu,p}|\chi_{\nu,p}[V]|^2 - N_D\right)$$

is equivalt to minimizing, under the constraints of the Schrödinger equation, the functional $P[V]$

$$P[V] = -\text{div}\left(\varepsilon_R \nabla V\right) + \frac{q}{\varepsilon_0}\left(\sum_{\nu,p}\rho_{\nu,p}|\chi_{\nu,p}[V]|^2 - N_D\right),$$

The scheme

which is achieved by means of a Newton scheme

$$dP(V^{old}, V^{new} - V^{old}) = -P[V^{old}].$$

The iterations

Derivatives

The Gâteaux-derivatives of the eigenproperties are needed:

$$
\begin{aligned}
d\epsilon_{\nu,p}(V, U) &= -q \int U(\zeta) |\chi_{\nu,p}[V](\zeta)|^2 d\zeta \\
d\chi_{\nu,p}(V, U) &= -q \sum_{p' \neq p} \frac{\int U(\zeta) \chi_{\nu,p}[V](\zeta) \chi_{\nu,p'}[V](\zeta) d\zeta}{\epsilon_{\nu,p}[V] - \epsilon_{\nu,p'}[V]} \chi_{\nu,p'}[V](z).
\end{aligned}
$$

Iterations

After computing the Gâteaux-derivative of the density and developping calculations, we are led to a Poisson-like equation

$$
-\mathrm{div}\left(\varepsilon_R \nabla V^{new}\right) + \int_0^{l_z} \mathcal{A}[V^{old}](z, \zeta) V^{new}(\zeta) d\zeta
$$

$$
= -\frac{q}{\varepsilon_0}\left(N[V^{old}] - N_D\right) + \int_0^{l_z} \mathcal{A}[V^{old}](z, \zeta) V^{old}(\zeta) d\zeta,
$$

where $\mathcal{A}[V]$ is essentially the Gâteaux-derivative of the functional $P[V]$.

The iterations

Derivatives

The Gâteaux-derivatives of the eigenproperties are needed:

$$
\begin{aligned}
d\epsilon_{\nu,p}(V,U) &= -q \int U(\zeta)|\chi_{\nu,p}[V](\zeta)|^2 d\zeta \\
d\chi_{\nu,p}(V,U) &= -q \sum_{p' \neq p} \frac{\int U(\zeta)\chi_{\nu,p}[V](\zeta)\chi_{\nu,p'}[V](\zeta)d\zeta}{\epsilon_{\nu,p}[V] - \epsilon_{\nu,p'}[V]} \chi_{\nu,p'}[V](z).
\end{aligned}
$$

Iterations

After computing the Gâteaux-derivative of the density and developping calculations, we are led to a Poisson-like equation

$$
-\mathrm{div}\,(\varepsilon_R \nabla V^{new}) + \int_0^{l_z} \mathcal{A}[V^{old}](z,\zeta)V^{new}(\zeta)d\zeta
$$
$$
= -\frac{q}{\varepsilon_0}\left(N[V^{old}] - N_D\right) + \int_0^{l_z} \mathcal{A}[V^{old}](z,\zeta)V^{old}(\zeta)d\zeta,
$$

where $\mathcal{A}[V]$ is essentially the Gâteaux-derivative of the functional $P[V]$.

| Introduction | Numerical methods | Benchmark tests | Diode | nanoMOSFET |
| 0000 | 000000000000 | 00000 | 000000000 | 0000000000 |

Solvers for Schrödinger and Poisson

Outline

Introduction	Numerical methods	Benchmark tests	Diode	nanoMOSFET
0000	000000000000	00000	000000000	0000000000

Solvers for Schrödinger and Poisson

Numerical methods

We need to solve the Schrödinger eigenvalue problem and Poisson equations.

The Schrödinger equation

Equation

$$-\frac{\hbar^2}{2}\frac{d}{dz}\left[\frac{1}{m_\nu}\frac{d\chi_{\nu,p}}{dz}\right] - q\left(V + V_c\right)\chi_{\nu,p} = \epsilon_{\nu,p}\chi_{\nu,p}$$

is discretized by alternate finite differences for the derivatives then the symmetric matrix is diagonalized by a LAPACK routine called DSTEQR.

The Poisson equation

We need to solve equations like

$$-\text{div}\left[\varepsilon_R \nabla V\right] + \int_0^{l_z} \mathcal{A}(z,\zeta)V(\zeta)d\zeta = \mathcal{B}(z).$$

The derivatives are discretized by finite differences in alternate directions, the integral is computed via trapezoid rule and the linear system (full) is solved by means of a LAPACK routine called DGESV.

| Introduction | Numerical methods | Benchmark tests | Diode | nanoMOSFET |
| 0000 | 000000000000 | 00000 | 000000000 | 0000000000 |

Solvers for Schrödinger and Poisson

Numerical methods

We need to solve the Schrödinger eigenvalue problem and Poisson equations.

The Schrödinger equation

Equation

$$-\frac{\hbar^2}{2}\frac{d}{dz}\left[\frac{1}{m_\nu}\frac{d\chi_{\nu,p}}{dz}\right] - q\left(V + V_c\right)\chi_{\nu,p} = \epsilon_{\nu,p}\chi_{\nu,p}$$

is discretized by alternate finite differences for the derivatives then the symmetric matrix is diagonalized by a LAPACK routine called DSTEQR.

The Poisson equation

We need to solve equations like

$$-\text{div}\left[\varepsilon_R \nabla V\right] + \int_0^{l_z} \mathcal{A}(z, \zeta)V(\zeta)d\zeta = \mathcal{B}(z).$$

The derivatives are discretized by finite differences in alternate directions, the integral is computed via trapezoid rule and the linear system (full) is solved by means of a LAPACK routine called DGESV.

Introduction	Numerical methods	Benchmark tests	Diode	nanoMOSFET
0000	000000000000	00000	000000000	0000000000

Solvers for Schrödinger and Poisson

Numerical methods

We need to solve the Schrödinger eigenvalue problem and Poisson equations.

The Schrödinger equation

Equation

$$-\frac{\hbar^2}{2}\frac{d}{dz}\left[\frac{1}{m_\nu}\frac{d\chi_{\nu,p}}{dz}\right] - q\left(V + V_c\right)\chi_{\nu,p} = \epsilon_{\nu,p}\chi_{\nu,p}$$

is discretized by alternate finite differences for the derivatives then the symmetric matrix is diagonalized by a LAPACK routine called DSTEQR.

The Poisson equation

We need to solve equations like

$$-\text{div}\left[\varepsilon_R \nabla V\right] + \int_0^{l_z} \mathcal{A}(z,\zeta)V(\zeta)d\zeta = \mathcal{B}(z).$$

The derivatives are discretized by finite differences in alternate directions, the integral is computed via trapezoid rule and the linear system (full) is solved by means of a LAPACK routine called DGESV.

Outline

Introduction	Numerical methods	Benchmark tests	Diode	nanoMOSFET
0000	000000000000	00000	000000000	0000000000

Experiments: simplifying assumptions

Collision operator

Results are presented for the the DG MOSFET in the one-valley, parabolic-band approximation. Moreover, the complete collision operator is substituted by a simple relaxation-time operator:

$$\mathcal{Q}_p f = \frac{1}{\tau} \left(\rho_p M - f_p \right).$$

The goal of this work is just the setting up of numerical tools for a more profound and realistic simulation.

A parallel code in the most realistic case is being implemented.

Thermodynamical equilibrium: one-valley case
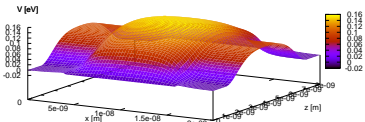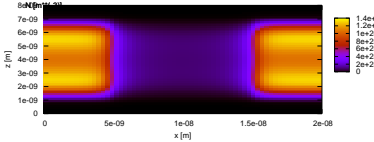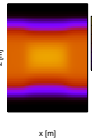
Introduction   Numerical methods   Benchmark tests   Diode   nanoMOSFET
0000   000000000000   00000   000000000   0000000000
Experiments: simplifying assumptions
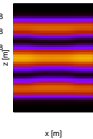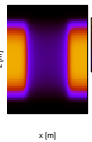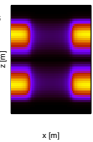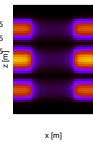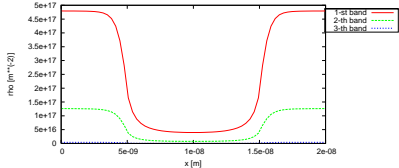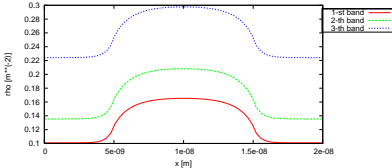
Transient states

We propose now some results relative to the long-time behavior of the system.